Civil and Environmental Research
ISSN 2224-5790 (Paper) ISSN 2225-0514 (Online)
Vol.8, No.10, 2016


# Behavior of Hybrid Reinforced Concrete Deep Beams under Repeated Loading

Sawsan Akram Hassan[1] Ghsoon Ali Faroun[2]*
1. Assist Prof. Dr., Civil Engineering Department, Al-Mustansiriayah University, Baghdad, Iraq
2. M.Sc. Student, Civil Engineering Department, Al-Mustansiriayah University, Baghdad, Iraq

**Abstract**
This research is devoted to investigate the experimental and theoretical behavior of hybrid deep beams under monotonic and repeated two points loading. The dimensions and the flexural reinforcement of the deep beams were kept constant. In this work, the idea of hybrid beam is completely different. Two types of concrete were used but not in cross section. The first type which is fiberous concrete (FC) was used in casting beam sides (shear spans), while the second type was conventional concrete (CC) which was used in the middle portion of beam (between two shear spans). This was done to strengthen the deep beam sides (shear spans) against cracking due to shear (diagonal strut) failure. The experimental program includes casting and testing of 12 deep beams, six of them are tested as a control beams under monotonic loading and the others were tested under repeated loading at level 70% of the ultimate load of their control beams. The variables include type of load, type of beam, amount of web reinforcement and amount of steel fiber. It was found when adding steel fiber to the shear spans by ratio 1% and 2% under monotonic loading system, the percentages increase in the ultimate load are 29.73% and 50.81%, respectively as compared with beam without steel fiber. Also, it was observed that when the entire deep beam cast with fiberous concrete, the percentages increase in the ultimate load are 5.21% as compared with hybrid beam with the same steel fiber ratio of 1%, and 36.49% as compared with deep beam cast with conventional concrete for all its portions. The increase in web reinforcement ratios from 0.0 to 0.003 and 0.004 under monotonic loading system leads to increase in the ultimate load are 34.08% and 42.46%, respectively. Comparison of experimental results was made with corresponding predicted values using the Strut and Tie procedure presented in Appendix A of ACI 318M-11Code and with other procedures mentioned in the literature. It was found that the Strut and Tie procedure presented in Appendix A of ACI 318M-11Code give conservative results as compared with the experimental tested results.
**Keywords:** deep beam, hybrid, repeated loading, strengthening, shear spans.

## 1. Introduction

Deep beams are structural members differ from slender beams in their geometrical proportions and nowadays are widely used in many structural applications such as transfer girders in multistory buildings, pile supported foundation, foundation walls, shear walls and bridges. Deep beam is defined as those members in which the ratio of effective span (Ln) to depth (h) is less than or equal to four ($Ln/h \leq 4$); or shear span (a) to depth (h) ratio less than or equal to two ($a/h \leq 2$) [1]. Reinforced concrete deep beams are typically used as transfer members in high-rise structures due to their high resistance capacity. Because the stress distribution in the section of the deep beam is nonlinear, the linear elastic theory for the general beam analysis cannot be applied. Therefore, ACI 318M-11Code requires that deep beams be designed via non-linear analysis or by Strut and Tie Models (STM) [2]. Hybrid concrete beams are characterized using different types of concrete specific layers for the purpose of increasing the resistance and improve performance.

## 2. Experimental Program

The experimental program consists of testing 12 simply supported deep beams under two point loads to investigate the behavior of reinforced concrete deep beams under repeated loading. All beams have the same dimensions and flexural reinforcement. They had an overall length of 1500 mm, a width of 150 mm and a height of 350 mm. The amount of flexural reinforcement for all the tested beams was 2Ø 20mm and 1Ø 16mm ($\rho = 0.0184$ where $\rho$ is the flexural reinforcement ratio). The clear span between supports was 1230 mm which results in a ratio of clear span to overall depth of 3.5. The variables include type of load, type of beam, amount of web reinforcement and amount of steel fiber. Also, bearing plates under each load and above each support were designed to avoid any local crushing in concrete. Table (1) show details of the fourteen tested reinforced concrete deep beams. The main parameters investigated and details of the web reinforcement are also shown. Details of dimension and reinforcement for each beam specimens are shown in Figure (1) to (3).

 

Table 1. Beam Specimens Details.

| *Beam No.* | *a/h* | *Type of Beams* | *Type of Load* | *Ratio of Steel Fiber* | *Vertical Web. Reinforced* | *Horizontal Web. Reinforced* | $\rho_w$ |
|---|---|---|---|---|---|---|---|
| **B1** | **1.14** | **Non-Hybrid (CC)** | **Monotonic** | **0%** | **Φ 4 mm @ 80 mm** | **Φ 4 mm @80 mm** | **0.003** |
| **B2** | **1.14** | **Non-Hybrid (CC)** | **Repeated (70%)** | **0%** | **Φ 4 mm @ 80 mm** | **Φ 4 mm @80 mm** | **0.003** |
| **B3** | **1.14** | **Non-Hybrid (FC)** | **Monotonic** | **1%** | **Φ 4 mm @ 80 mm** | **Φ 4 mm @80 mm** | **0.003** |
| **B4** | **1.14** | **Non-Hybrid (FC)** | **Repeated (70%)** | **1%** | **Φ 4 mm @ 80 mm** | **Φ 4 mm @80 mm** | **0.003** |
| **B5** | **1.14** | **Hybrid** | **Monotonic** | **1%** | **Φ 4 mm @ 80 mm** | **Φ 4 mm @80 mm** | **0.003** |
| **B6** | **1.14** | **Hybrid** | **Repeated (70%)** | **1%** | **Φ 4 mm @ 80 mm** | **Φ 4 mm @80 mm** | **0.003** |
| **B7** | **1.14** | **Hybrid** | **Monotonic** | **1%** | **-** | **-** | **0.0** |
| **B8** | **1.14** | **Hybrid** | **Repeated (70%)** | **1%** | **-** | **-** | **0.0** |
| **B9** | **1.14** | **Hybrid** | **Monotonic** | **1%** | **Φ 4 mm @ 60 mm** | **Φ 4 mm @60 mm** | **0.004** |
| **B10** | **1.14** | **Hybrid** | **Repeated (70%)** | **1%** | **Φ 4 mm @ 60 mm** | **Φ 4 mm @60 mm** | **0.004** |
| **B11** | **1.14** | **Hybrid** | **Monotonic** | **2%** | **Φ 4 mm @ 80 mm** | **Φ 4 mm @80 mm** | **0.003** |
| **B12** | **1.14** | **Hybrid** | **Repeated (70%)** | **2%** | **Φ 4 mm @ 80 mm** | **Φ 4 mm @80 mm** | **0.003** |

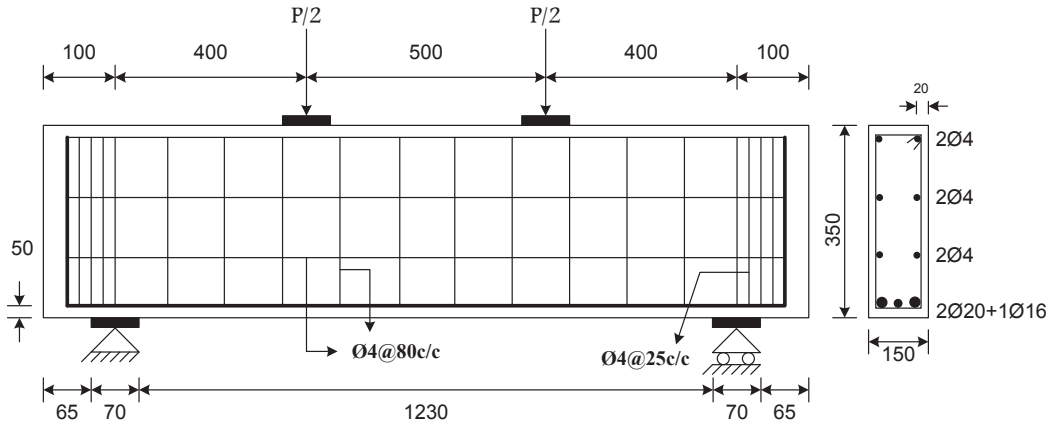


Figure 1. Details of Beams (B1, B2, B3, B4, B5, B6, B11, B12) (All Dimensions are in mm).

 

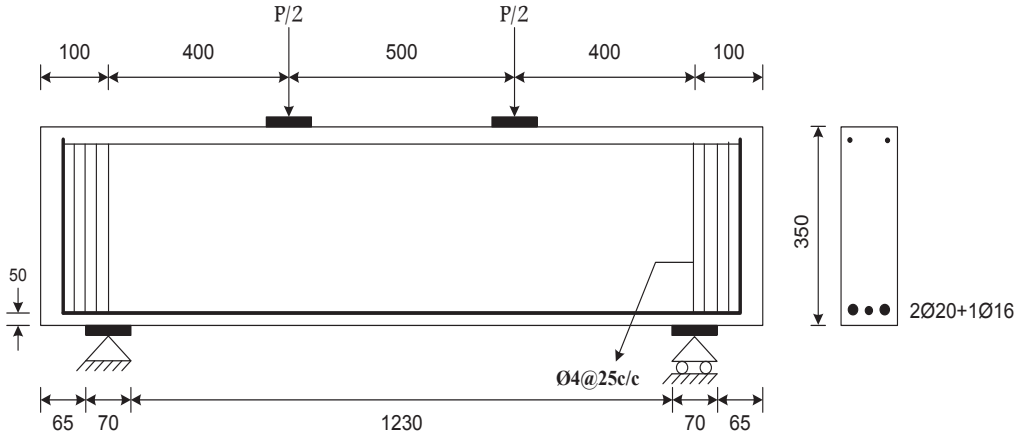


Figure 2. Details of Beams (B7, B8) (All Dimensions are in mm).

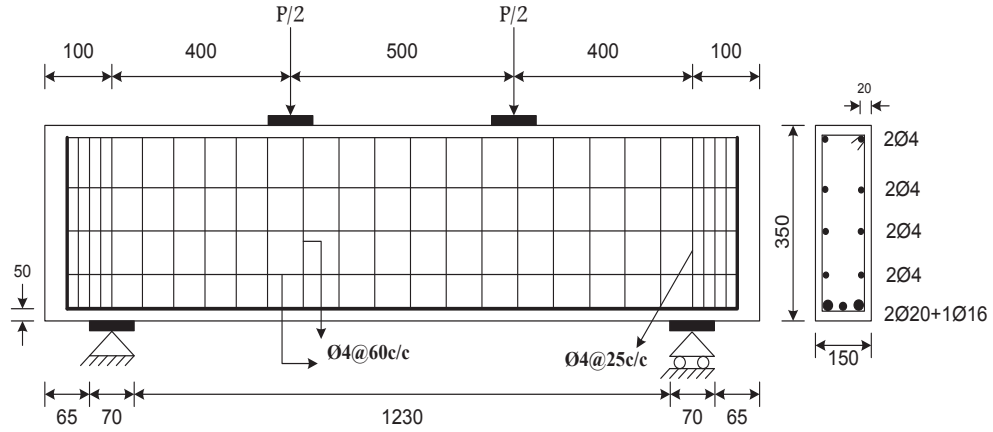


Figure 3. Details of Beams (B9, B10) (All Dimensions are in mm).

*2.1 Materials*

Properties and description of used materials are reported and presented in Table (2) and the concrete mix proportions are reported and presented in Table (3).

Table 2. Properties of Construction Materials.

| ***Material*** | ***Descriptions*** |
|---|---|
| **Cement** | **Ordinary Portland Cement (Type I)** |
| **Sand** | **Natural sand from Al-Ukhaider region with maximum size of (4.75mm)** |
| **Gravel** | **Crushed gravel of maximum size (19 mm)** |
| **Steel Fiber** | **Hooked ends mild steel fibers are used in construction of fiberous concrete with volumetric ratio (*vf*) of 0%, 1% and 2%.** |
| **Reinforcing Bars** | **(ϕ20mm) deformed steel bar, having (630MPa) yield strength (fy)**<br>**(ϕ16mm) deformed steel bar, having (780MPa) yield strength (fy)**<br>**(ϕ4mm) plane steel bar, having (540MPa) yield strength (fy)** |
| **Water** | **Clean tap water** |

Table 3. Proportions of Concrete Mix.

| ***Compressive Strength (MPa)*** | ***Cement ($kg/m^3$)*** | ***Sand ($kg/m^3$)*** | ***Gravel ($kg/m^3$)*** | ***Water Cement ratio w/c*** | ***Steel Fiber (%)*** | ***Steel Fiber ($kg/m^3$)*** |
|---|---|---|---|---|---|---|
| **30** | **400** | **728** | **1092** | **0.5** | **0** | **-** |
| | | | | | **1** | **78** |
| | | | | | **2** | **156** |

 

*2.2 Description of Reinforcement Bars*

The horizontal length of all longitudinal reinforcement was 1460 mm and a vertical length of 250mm to make a $90^{\circ}$ standard hook to provide sufficient anchorage as shown in Plate (1).

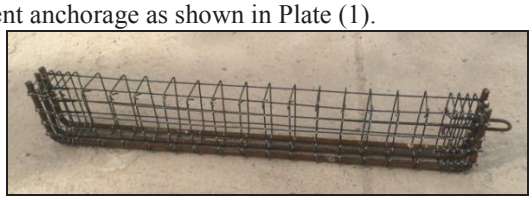

Plate 1. Steel Reinforcement Cage Used for Deep Beams.

*2.3 Molds and Casting*

Two steel molds were designed and fabricated for casting two hybrid deep beams for each batch. The inside dimensions for each mold were 1500mm ×150mm ×350mm (length × width × depth). The molds were fabricated to cast the beams vertically due to the difficulty of casting layers in horizontal state. The front cover of the mold face of dimensions (1500mm×350mm) consists of three Plates. The lower plate was fixed to cast the first layer while the two other plates above were movable (doors) to cast the two other layers. Each door was closed before casting the layer of beam backwards it. The molds were placed in vertical position and all reinforcing bars were previously prepared. The reinforcement cage then put in position. Details of molds and casting procedure are shown in Plate (2).

Plate 2. Details of Molds and Casting Procedure.

*2.4 Test Procedure*

All beam specimens and control specimens have been removed from curing at the age of 28 days. Before the testing day, the beam specimens have been cleaned and paint with white paint in order to clarify the crack propagation. Each beam specimen has been labeled and the locations of support points, loading points and the dial gauge position were marked on the surface of beam. The beam specimens have been placed on the machine with a clear span (1230mm), as shown in Plates (3). The marked loading points have been covered by (150×70×40) mm steel plates to avoid stress concentrations on the upper face of the beams during loading. All beam specimens have been tested under two points load. The dial gauge was mounted in their marked position to touch the bottom of center of the beams was fixed in the correct location. All beam specimens have been loaded to failure in one cycle for monotonic test and 5 cycles in repeated loading test. The beam specimens have been loaded in increments of (10kN), the rate of load increment was about (1.5kN/sec). The positions and extents of consequent cracks for each cycle were marked on the surface of the beam. As failure occurred, when the beam failed abruptly at simultaneity with the load indicator stopped in recording or return back and the deflection increased very fast. The failure load has been recorded, and the hydraulic load has been removed.

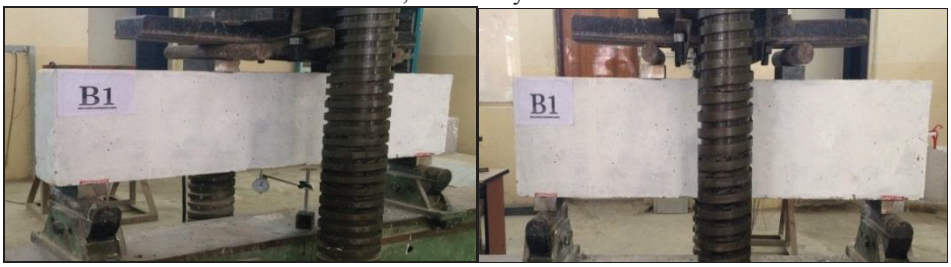


a.Side View for Beam (B1) under Testing. b. Front View for Beam (B1) under Testing.

Plate 3. Test Procedure for Beam Specimen.

 

## 3. Experimental Results

In monotonic loading, during the applied load and at the low load level, all the tested beams behaved in an elastic manner and the deflection at mid span were small proportion to the applied loads. When the load was increased, first crack was occur, then number of cracks were observed at the region of the pure bending moment. At repeated loading when deep beam specimens were subjected to applied load, similar cracks that which occurred in monotonic test were observed at first cycle. At next cycles, the same cracks that were observed at the first cycle during loading phase were gradually widened and propagated diagonally along the main strut, at the last cycle, beams loaded up to failure. Finally, failure occurred by splitting the inclined line joining the edge of steel plates at the supports and loading positions (strut of the deep beam) except for beam B11 which failed in flexural mode (crushing compression chord). Details of the tested beams and results obtained are shown in Table (4).

Table 4. Summary of Test Results for Tested Deep Beams*.

| *Beam No.* | *Beam Type* | $\rho_w$ ** | *Steel Fiber Ratio (SF)* | *Type of Loading* | *No. of Cycles* | *Ultimate Load (kN)* | *Modes of Failure* |
|---|---|---|---|---|---|---|---|
| **B1** | **Non-Hybrid (CC)** | **0.003*** (Min)** | **0%** | **Monotonic** | **-** | **370** | **Diagonal Shear Failure** |
| **B2** | **Non-Hybrid (CC)** | **0.003 (Min)** | **0%** | **Repeated (70% of B1 Ultimate Load)** | **5** | **293** | **Diagonal Shear Failure** |
| **B3** | **Non-Hybrid (FC)** | **0.003 (Min)** | **1%** | **Monotonic** | **-** | **505** | **Diagonal Shear Failure** |
| **B4** | **Non-Hybrid (FC)** | **0.003 (Min)** | **1%** | **Repeated (70% of B3 Ultimate Load)** | **5** | **410** | **Diagonal Shear Failure** |
| **B5** | **Hybrid** | **0.003 (Min)** | **1%** | **Monotonic** | **-** | **480** | **Diagonal Shear Failure** |
| **B6** | **Hybrid** | **0.003 (Min)** | **1%** | **Repeated (70% of B5 Ultimate Load)** | **5** | **350** | **Diagonal Shear Failure** |
| **B7** | **Hybrid** | **0.0** | **1%** | **Monotonic** | **-** | **358** | **Diagonal Shear Failure** |
| **B8** | **Hybrid** | **0.0** | **1%** | **Repeated (70% of B7 Ultimate Load)** | **5** | **351** | **Diagonal Shear Failure** |
| **B9** | **Hybrid** | **0.004 (>Min)** | **1%** | **Monotonic** | **-** | **510** | **Diagonal Shear Failure** |
| **B10** | **Hybrid** | **0.004 (>Min)** | **1%** | **Repeated (70% of B9 Ultimate Load)** | **5** | **390** | **Diagonal Shear Failure** |
| **B11** | **Hybrid** | **0.003 (Min)** | **2%** | **Monotonic** | **-** | **558** | **Shear-Flexural Failure** |
| **B12** | **Hybrid** | **0.003 (Min)** | **2%** | **Repeated (70% of B11 Ultimate Load)** | **5** | **418** | **Diagonal Shear Failure** |

* All beams have the same (a/h) ratio = 1.14

** $\rho_w = \Sigma \frac{A_{st}}{b_w s_i} sin_{\alpha_i}$

*** Min web reinforcement ratio = 0.003 for all tested beams.

Plates (4) to (15) show modes of failure and the crack patterns of the tested deep beams.

 

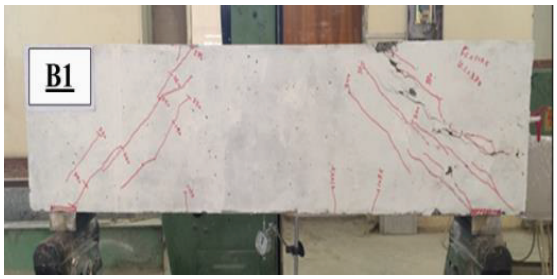

Plate 4. Crack Pattern for Beam B1 after Testing.

Plate 5. Crack Pattern for Beam B2 after Testing.

Plate 6. Crack Pattern for Beam B3 after Testing.

Plate 7. Crack Pattern for Beam B4 after Testing.

Plate 8. Crack Pattern for Beam B5 after Testing.

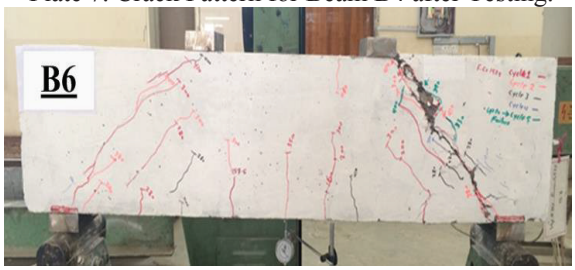

Plate 9. Crack Pattern for Beam B6 after Testing.

Plate 10. Crack Pattern for Beam B7 after Testing.

Plate 11. Crack Pattern for Beam B8 after Testing.

Plate 12. Crack Pattern for Beam B9 after Testing.

Plate 13. Crack Pattern for Beam B10 after Testing.

 

Plate 14. Crack Pattern for Beam B11 after Testing.

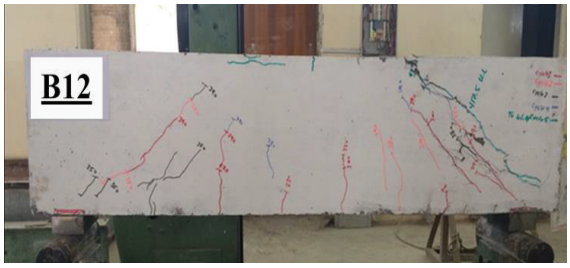

Plate 15. Crack Pattern for Beam B12 after Testing.

*3.1 Effect of Loading Type*

Table (5) illustrate the effect of loading type, monotonic or repeated with load level 70%, on ultimate load of hybrid or non-hybrid tested deep beams.

Table 5. Effect of Loading Type for All Tested Deep Beams.

| *Beam No.* | *Beam Type* | $\rho_w$ | *SF Ratio* | *Type of Loading* | *No. of Cycles* | *Ultimate Load (kN)* | *Percentage decrease (%)* |
|---|---|---|---|---|---|---|---|
| **B1** | **Non-Hybrid (CC)** | **0.003** | **0%** | **Monotonic (Control)** | **-** | **370** | **20.81** |
| **B2** | **Non-Hybrid (CC)** | **0.003** | **0%** | **Repeated (70% of Control Beam Load)** | **5** | **293** | |
| **B3** | **Non-Hybrid (FC)** | **0.003** | **1%** | **Monotonic (Control)** | **-** | **505** | **18.81** |
| **B4** | **Non-Hybrid (FC)** | **0.003** | **1%** | **Repeated (70% of Control Beam Load)** | **5** | **410** | |
| **B5** | **Hybrid** | **0.003** | **1%** | **Monotonic (Control)** | **-** | **480** | **27.08** |
| **B6** | **Hybrid** | **0.003** | **1%** | **Repeated (70% of Control Beam Load)** | **5** | **350** | |
| **B7** | **Hybrid** | **0.0** | **1%** | **Monotonic (Control)** | **-** | **358** | **1.96** |
| **B8** | **Hybrid** | **0.0** | **1%** | **Repeated (70% of Control Beam Load)** | **5** | **351** | |
| **B9** | **Hybrid** | **0.004** | **1%** | **Monotonic (Control)** | **-** | **510** | **23.53** |
| **B10** | **Hybrid** | **0.004** | **1%** | **Repeated (70% of Control Beam Load)** | **5** | **390** | |
| **B11** | **Hybrid** | **0.003** | **2%** | **Monotonic (Control)** | **-** | **558** | **25.09** |
| **B12** | **Hybrid** | **0.003** | **2%** | **Repeated (70% of Control Beam Load)** | **5** | **418** | |
| | | | | | | | **X' = 23.06** |

From observation of Table (5), the following points can be noticed:

1- The percentages decrease in ultimate load according to repeated loading for non-hybrid deep beams of CC and FC is convergent which are (20.81% and 18.81%), respectively.

2- The percentages decrease in ultimate load according to repeated loading which have SF ratio of (1% and 2%) as variable is convergent (27.08% and 25.09%), respectively.

3- The percentages decrease in ultimate load according to repeated loading which have web reinforcement of (0.003 and 0.004) as variable is convergent (27.08% and 23.53%), respectively.

4- The percentages decrease between the hybrid deep beams without web reinforcement when subjected to monotonic and repeated loading is of negligible value (1.96%).

5- The mean value of the percentages decrease of beams subjected to monotonic and 70% repeated loading is (23.06%) excluding the percentage decease of beams without web reinforcement since it is far from all other values (abnormal).

 

*3.2 Effect of Beam Type*

3.2.1 under Monotonic Load

Effects of this variable are shown in Figure (4) and Table (6). Beam B1 was cast using CC, while beam B5 was cast using CC at mid region and FC at sides, finally beam B3 was cast using FC.

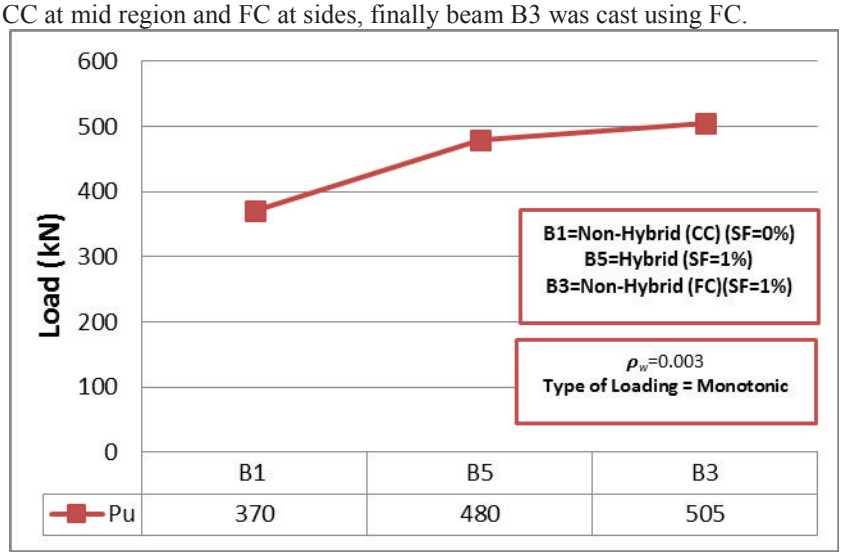


Figure 4. Effect of Beam Type on Ultimate Load under Monotonic Loading.

Table 6. Effect of Beam Type on Ultimate Load under Monotonic Loading.

| *Beam No.* | *Beam Type* | *SF Ratio* | *$\rho_w$* | *Ultimate Load (Pu) (kN)* | *% Increase Ultimate Load ** |
|---|---|---|---|---|---|
| **B1** | **Non- Hybrid (CC)** | **0%** | **0.003** | **370** | **-** |
| **B5** | **Hybrid** | **1%** | **0.003** | **480** | **29.73%** |
| **B3** | **Non- Hybrid (FC)** | **1%** | **0.003** | **505** | **36.49%**** |

*The percentage increase is measured with respect to beam B1.

** The percentage increase of load of beam B3 is (5.21) with respect to beam B5.

The increase in ultimate load for B3 and B5 are about 36.49% and 29.73% respectively, with respect to B1. Through this results, it observed that the addition of a moderate proportion of SF (1%) to beam shear spans (B5) lead to improve the amount of resistance by a significant ratio of (29.73%), while when the same proportion of SF was added through the entire length of the beam (B3) the percent of increase is also significant (36.49%) but slightly higher than the hybrid beam with SF only at shear spans (5.21%). It can be concluded that the presence of SF ratio in the region of pure bending is insignificant in deep beams subjected to monotonic loading.

3.2.2 under Repeated Loading

Results shown in Figure (5) and listed in Table (7) show the effect of the variable beam type on ultimate load for deep beams tested under repeated loading by 70% of ultimate monotonic loading of similar beams.

 

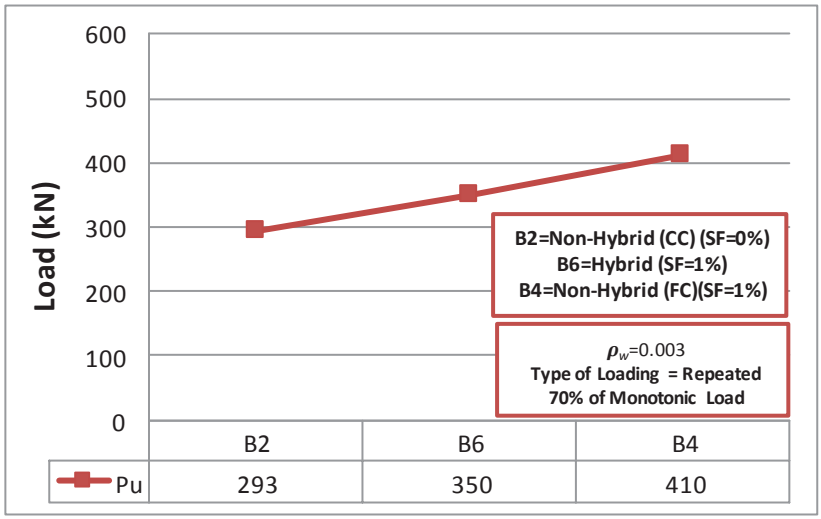


Figure 5. Effect of Beam Type on Ultimate Load under Repeated Loading.

Table 7. Effect of Beam Type on Ultimate Load under Repeated Loading.

| *Beam No.* | *Beam Type* | *SF Ratio* | *$\rho_w$* | *Ultimate Load (Pu) (kN)* | *% Increase Ultimate Load ** |
|---|---|---|---|---|---|
| **B2** | **Non- Hybrid (CC)** | **0%** | **0.003** | **293** | **-** |
| **B6** | **Hybrid** | **1%** | **0.003** | **350** | **19.45%** |
| **B4** | **Non- Hybrid (FC)** | **1%** | **0.003** | **410** | **39.93%**** |

*The percentage increase is measured with respect to beam B2.

**The percentage increase of load of beam B4 is (17.14) with respect to beam B6.

From observation of results of Table (7), it can be seen that the hybrid beam (B6) fails in load higher than non-hybrid beam cast from CC by (19.45%), while beam (B4) which was cast from FC (SF1%) fails in load significantly higher than the two beams (B2 and B7). The percentage increase in ultimate load of beam B4 is (17.14%) with respect to beam B6. Figure (6) shows the effect of beam type under monotonic and repeated loading. It can be concluded that the presence of SF in the region of pure bending in beams subjected to repeated loading level of 70% of monotonic ultimate load of similar beams are considerable importance as compared to similar beams subjected to monotonic loading.

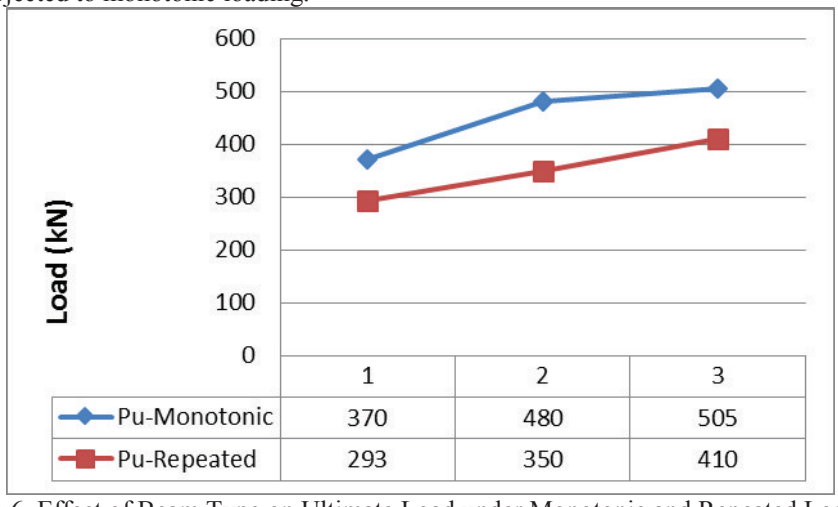


Figure 6. Effect of Beam Type on Ultimate Load under Monotonic and Repeated Loading.

*3.3 Effect of SF Ratio*

3.3.1 under Monotonic Load

Figure (7) and results in Table (8) show the effect of ratio of SF ratio on ultimate loads for deep beams that tested under monotonic loading.

 

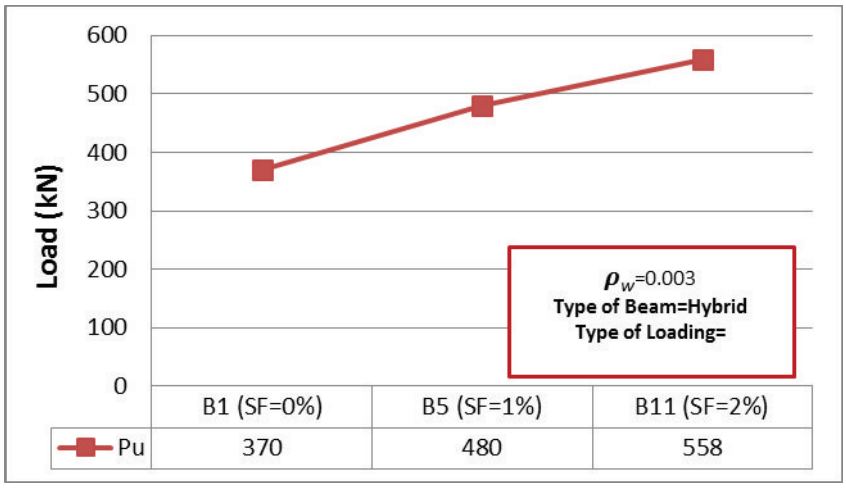


Figure 7. Effect of SF Ratio on Ultimate Load of Beams under Monotonic Loading.

Table 8. Effect of SF Ratio on Ultimate Load of Beams under Monotonic Loading.

| *Beam No.* | *Beam Type* | *SF Ratio* | *$\rho_w$* | *Ultimate Load (Pu) (kN)* | *% Increase Ultimate Load ** |
|---|---|---|---|---|---|
| **B1** | **Non-Hybrid** (CC)** | **0%** | **0.003** | **370** | **-** |
| **B5** | **Hybrid** | **1%** | **0.003** | **480** | **29.73%** |
| **B11** | **Hybrid** | **2%** | **0.003** | **558** | **50.81%** |

*The percentage increase is measured with respect to beam B1.
**Hybrid beam with SF ratio = 0%.

The ultimate load for hybrid beam with SF ratio of 2% (B11) and SF ratio of 1% (B5) increased by 50.81% and 29.73%, respectively with respect to B1with 0% SF ratio. The presence of SF in shear span region for hybrid deep beams contribute in enhancing resistance of hybrid deep beams and improve its performance.

3.3.2 under Repeated Loading

Figure (8) and Table (9) show the effect of SF ratio on ultimate load of hybrid deep beams tested under repeated loading level of 70% of control monotonic loading.

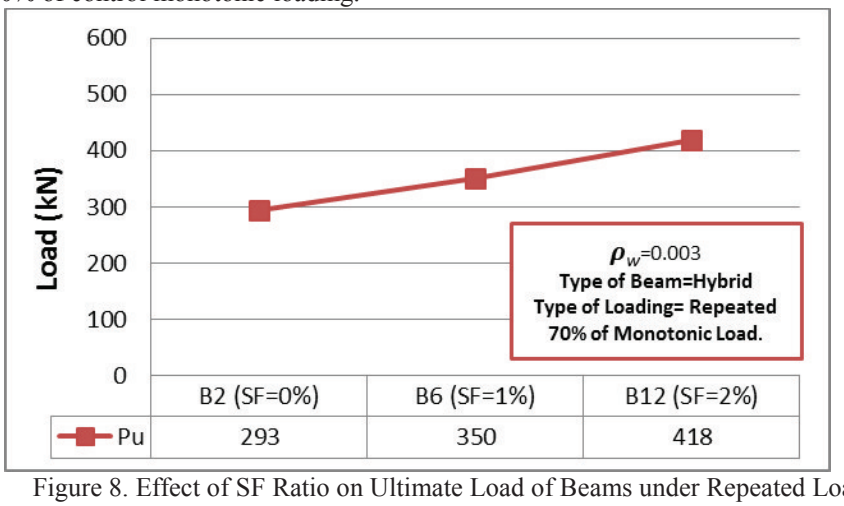


Figure 8. Effect of SF Ratio on Ultimate Load of Beams under Repeated Loading.

 

Table 9. Effect of SF Ratio on Ultimate Load of Beams under Repeated Loading.

| *Beam No.* | *Beam Type* | *SF Ratio* | $\rho_w$ | *Ultimate Load (Pu) (kN)* | *% Increase Ultimate Load ** |
|---|---|---|---|---|---|
| **B2** | **Non-Hybrid** (CC)** | **0%** | **0.003** | **293** | **-** |
| **B6** | **Hybrid** | **1%** | **0.003** | **350** | **19.45%** |
| **B12** | **Hybrid** | **2%** | **0.003** | **418** | **42.66%** |

*The percentage of increase is measured with respect to beam B2.
**Hybrid beam with SF ratio = 0%.

From the observation of results in Table (9) it was found that SF ratio in hybrid beams under repeated loading is significant. The capacity of hybrid deep beams with ratio of SF 2% and 1% are increased by about 42.66% and 19.45%, respectively with respect to B2. Figure (9) show the effect of SF ratio on ultimate load of hybrid deep beams under monotonic and repeated loading.

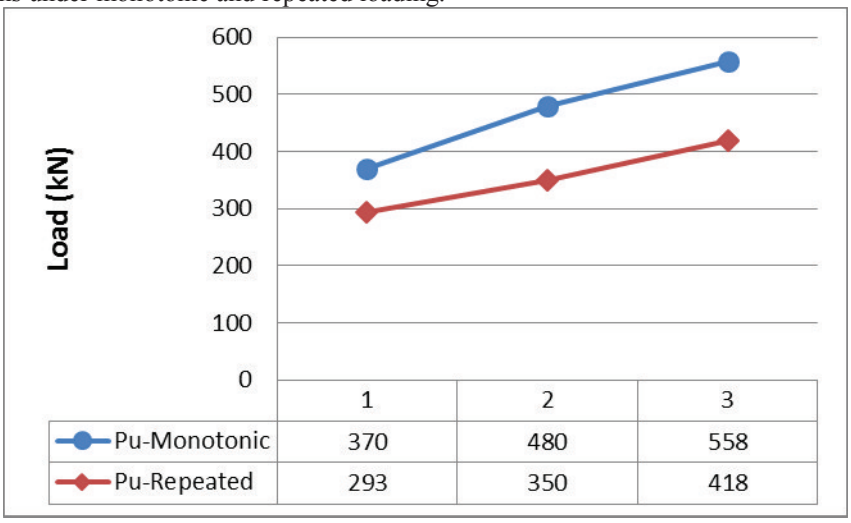


Figure 9. Effect of SF Ratio on Ultimate Load of Beams under Monotonic and Repeated Loading.

*3.4. Effect of Web Reinforcement Ratio ($\rho_w$)*

3.4.1under Monotonic Loading

The results are drawn in Figure (10) and also listed in Table (10).

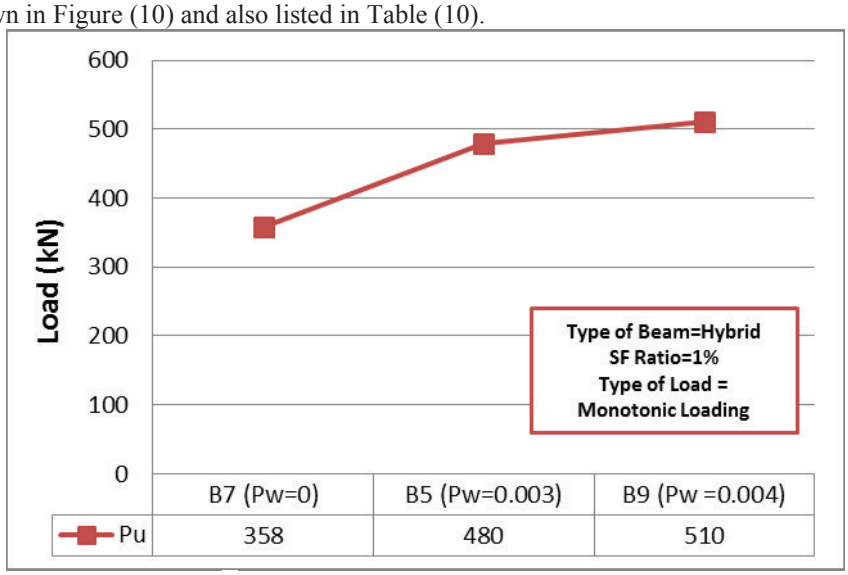


Figure 10. Effect of $\rho_w$ on Ultimate Load of Beams under Monotonic Loading.

 

Table 10. Effect of $\rho_w$ on Ultimate Load of Beams under Monotonic Loading.

| *Beam No.* | *Beam Type* | *SF Ratio* | $\rho_w$ | *Ultimate Load (Pu) (kN)* | *% Increase Ultimate Load ** |
|---|---|---|---|---|---|
| **B7** | **Hybrid** | **1%** | **0.0** | **358** | **-** |
| **B5** | **Hybrid** | **1%** | **0.003** | **480** | **34.08%** |
| **B9** | **Hybrid** | **1%** | **0.004** | **510** | **42.46%** |

*The percentage of increase is measured with respect to beam B7.

From the results it can be seen that the increase in ultimate loads are 34.08% and 42.46%, respectively as the ratio of web reinforcement increased from (0 to 0.003) and from (0 to 0.004).

3.4.2 under Repeated Loading

The effect of web reinforcement ratio on ultimate load for hybrid deep beams under repeated loading are shown in Figure (11) and listed in Table (11).

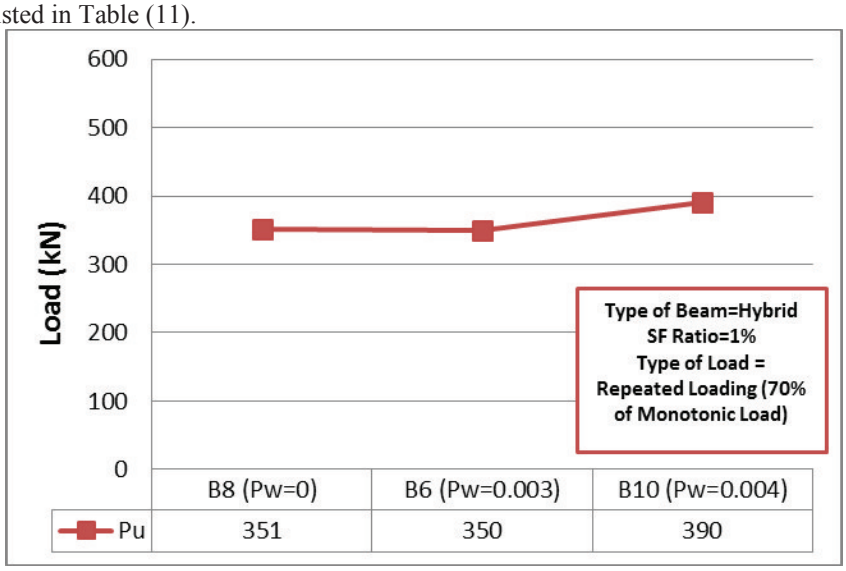


Figure 11. Effect of $\rho_w$ on Ultimate Load of Beams under Repeated Loading.

Table 11. Effect of $\rho_w$ on Ultimate Load of Beams under Repeated Loading.

| *Beam No.* | *Beam Type* | *SF Ratio* | $\rho_w$ | *Ultimate Load (Pu) (kN)* | *% Increase Ultimate Load ** |
|---|---|---|---|---|---|
| **B8** | **Hybrid** | **1%** | **0.0** | **351** | **-** |
| **B6** | **Hybrid** | **1%** | **0.003** | **350** | **-0.00%** |
| **B10** | **Hybrid** | **1%** | **0.004** | **390** | **11.11%** |

*The percentage of increase is measured with respect to beam B8.

From observation of Figure (11) and Table (11), it can be seen that there is no increase in the value of ultimate load as $\rho_w$ increase from (0 to 0.003) which is minimum reinforcement ratio while there is an increase in ultimate load value of (11.11%) as the $\rho_w$ increased from (0 to 0.004).

Figure (12) show the effect of $\rho_w$ on ultimate load of hybrid deep beams as they subjected to monotonic loading and repeated loading of level 70% of control beam monotonic ultimate load. It can be seen that the ultimate load show significant increase as compared to repeated loading which suffers slight increase when $\rho_w$ increased from (0 to 0.004).

 

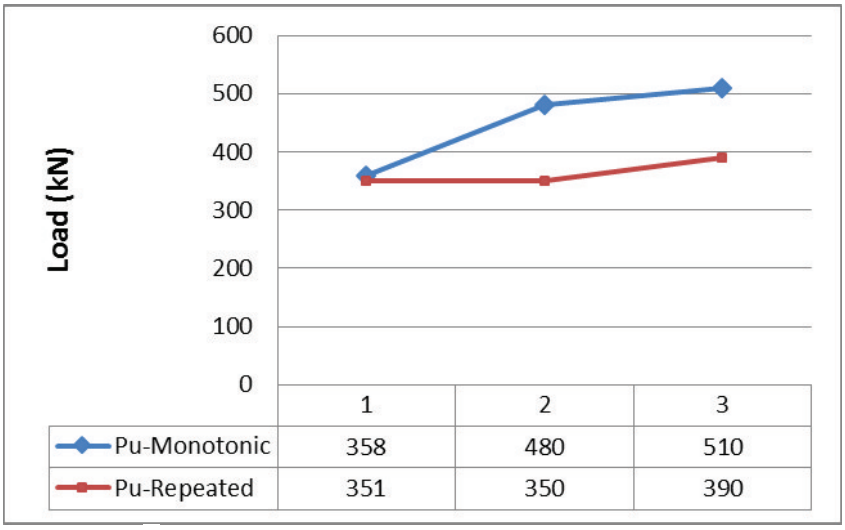


Figure 12. Effect of $\rho_w$ on Ultimate Load of Beams under Monotonic and Repeated Loading.

*3.5 Load-Deflection Response*

Figures (13) through (24), show the load mid-span deflection curves obtained for the all tested deep beam specimens which were tested under monotonic and repeated loading. The load mid-span deflection curves are initiated in a linear form with a constant slope. After initiating cracks, the load- deflection response takes a nonlinear form with variable slope where the deflection is increased at an increasing rate as the applied load is increased. The load mid-span deflection curves appeared to be dependent on type of loading, type of beam, different SF ratio and amount of web reinforcement.

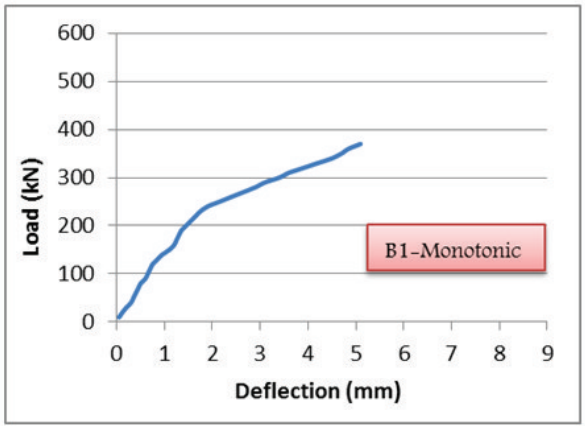


Figure 13. Load mid-span Deflection for Beam B1.

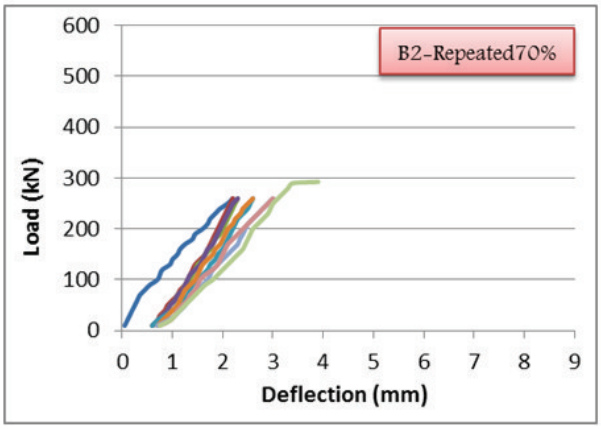


Figure 14. Load mid-span Deflection for Beam B2.

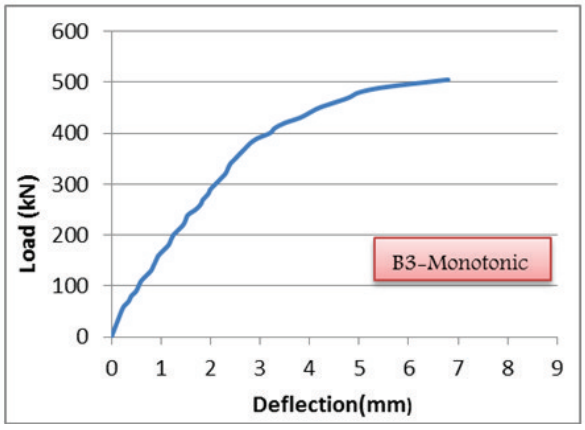


Figure 15. Load mid-span Deflection for Beam B3.

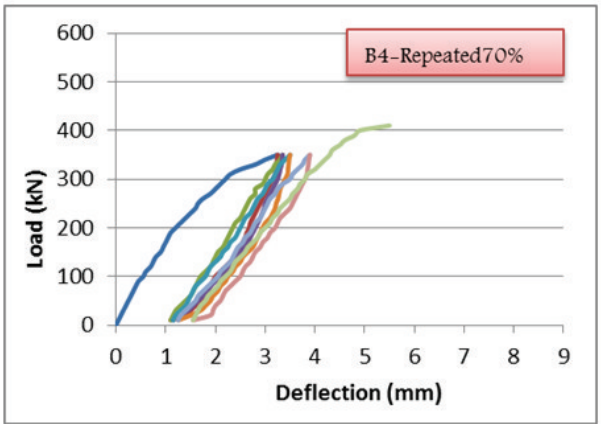


Figure 16. Load mid-span Deflection for Beam B4.

 

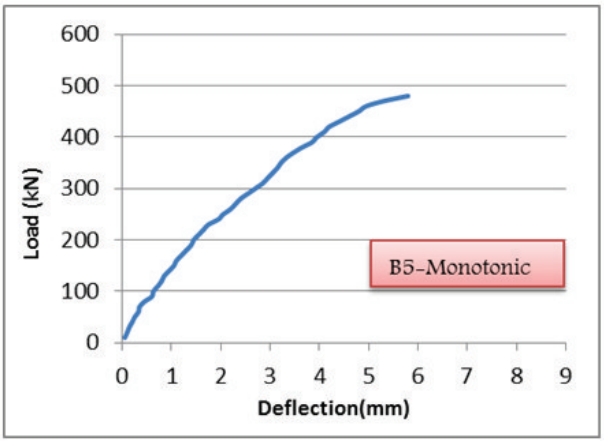


Figure 17. Load mid-span Deflection for Beam B5.

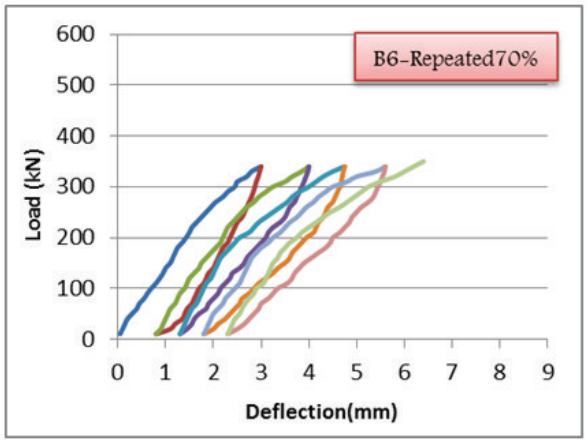


Figure 18. Load mid-span Deflection for Beam B6.

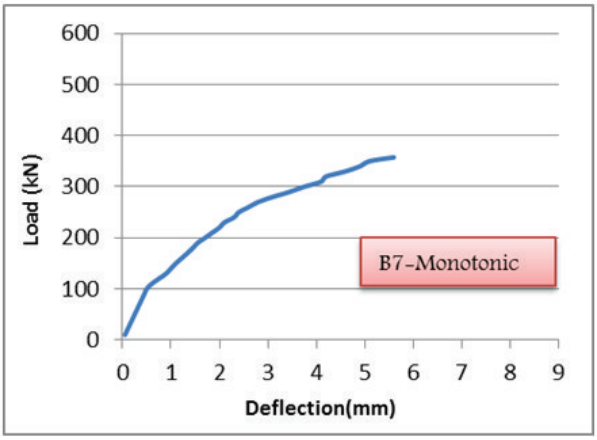


Figure 19. Load mid-span Deflection for Beam B7.

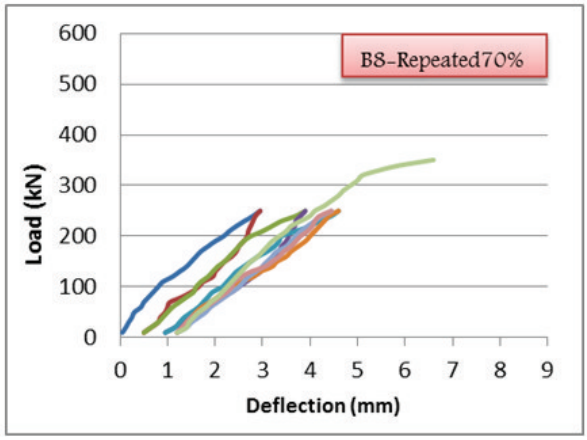


Figure 20. Load mid-span Deflection for Beam B8.

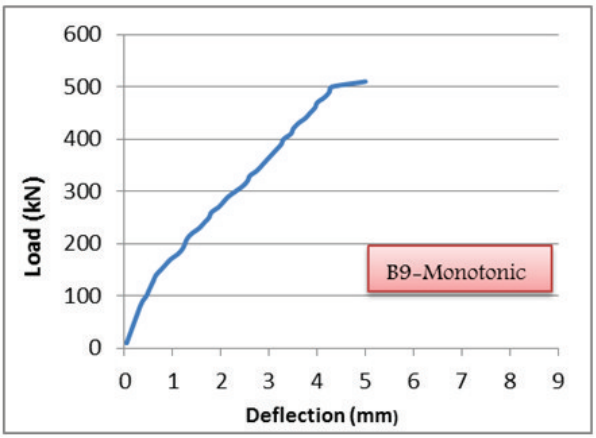


Figure 21. Load mid-span Deflection for Beam B9.

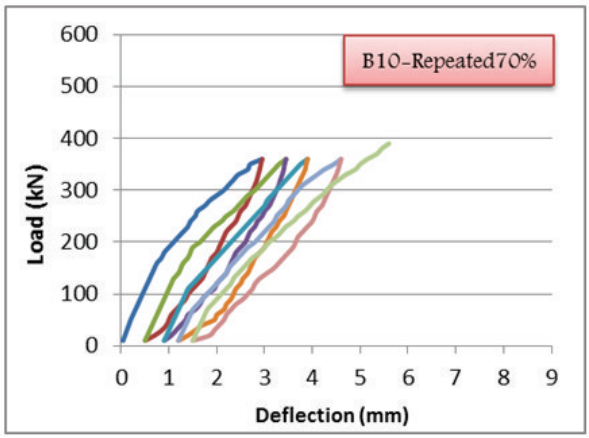


Figure 22. Load mid-span Deflection for Beam B10.

 

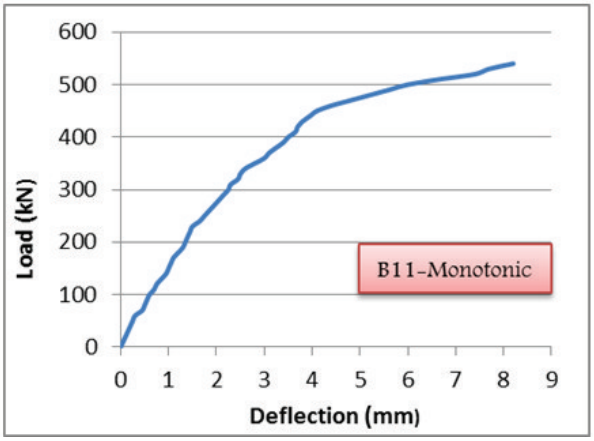


Figure 23. Load mid-span Deflection for Beam B11.

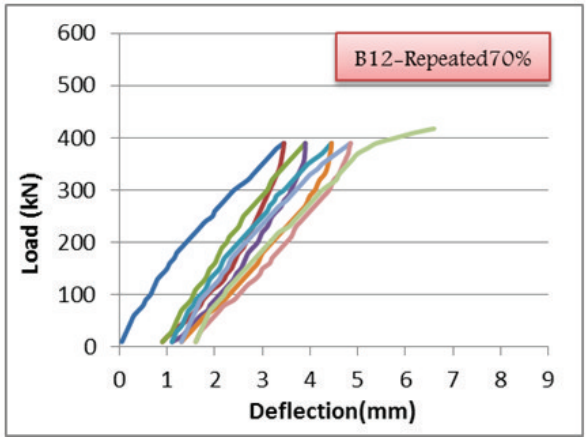


Figure 24. Load mid-span Deflection for Beam B12.

3.5.1 Effect of Type of Beam

Figure (25) shows the difference between load mid-span deflection responses of beams (beam B1 (CC), beam B5 (hybrid beam with SF ratio 1% in shear span and beam B3 (FC)) under monotonic loading.

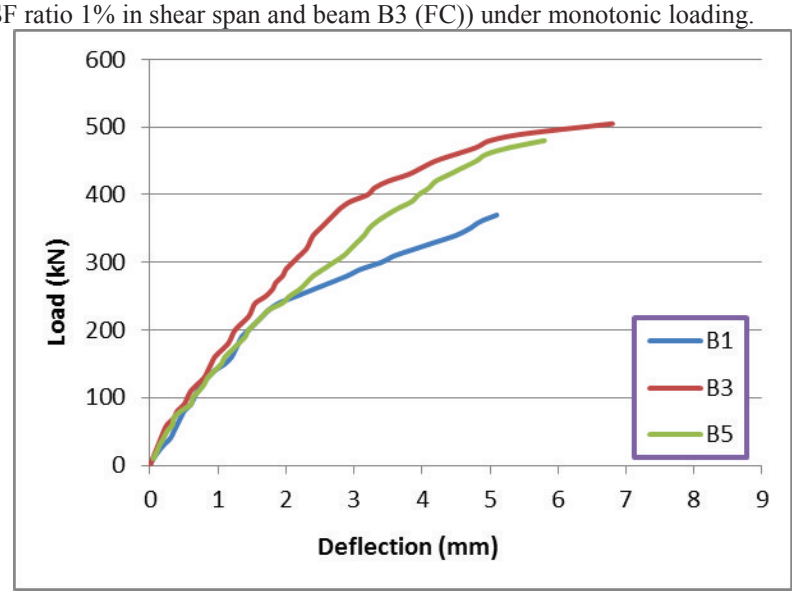


Figure25. Load mid-span Deflection Response for Different Beam Types under Monotonic Loading.

3.5.2 Effect of SF Ratios

Figure (26) show the effect addition of SF for hybrid deep beams on load mid-span deflection response under monotonic loading. Three volumetric ratios of SF were used. Hybrid beam with SF ratio of 2% have the smaller deflection values at each stage of loading compared to other beams that have SF ratios of 1% and 0%.

 

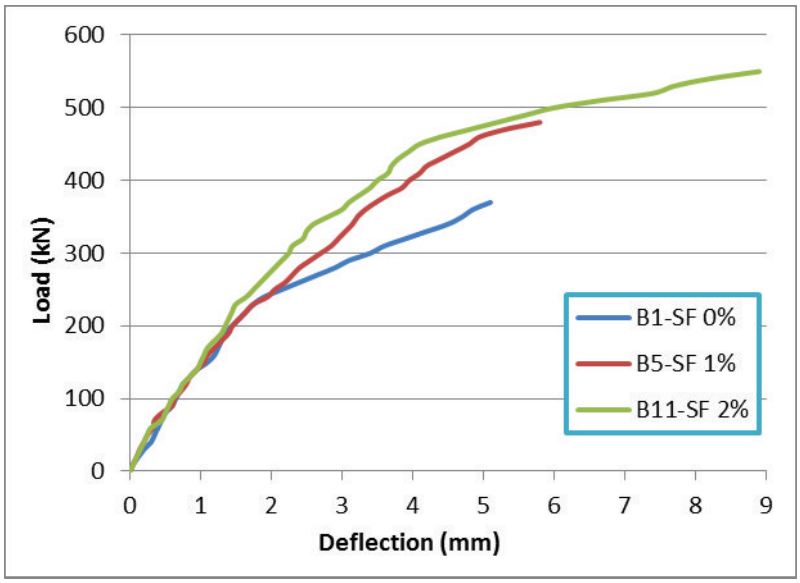


Figure 26. Load mid-span Deflection Response for Hybrid Beams with Different SF Ratios under Monotonic Loading.

3.5.3 Effect of Web Reinforcement Ratio

Adding web reinforcement in different amounts contributed effectively to improving the performance of beams. Figure (27) show effect of $\rho_w$ on load mid-span deflection for beams (controls) that which tested under monotonic loading.

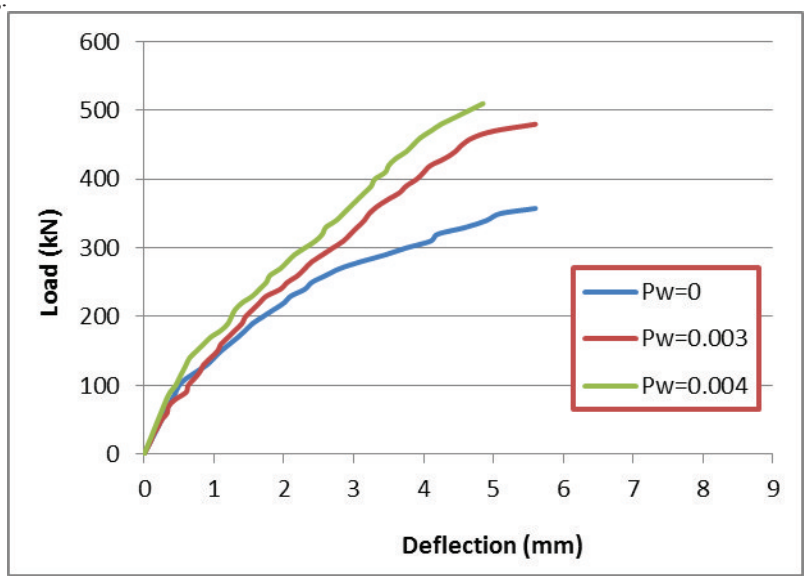


Figure 27. Load mid-span Deflection for Hybrid Beams with Different $\rho_w$ Ratios under Monotonic Loading.

## 4. Theoretical Program

The Strut and Tie modeling (STM) technique is a widely accepted design approach for reinforced concrete deep beams. Where geometrical discontinuity exists in structural members, current code documents provide little direction for design. The design of these structural concrete members can be better understood by using STM [3]. In this work, three methods will be used to predict ultimate load of simply supported deep beams tested under two point monotonically loading system which are:

1. Strut and tie model according to ACI 318M-11Code procedure.
2. Modified strut and tie method proposed by Zhang and Tan in March 2007.
3. Modified strut and tie model proposed by Zhang and Tan in November 2007, which takes into account size effect of reinforced concrete deep beams.

*4.1 Theory of STM*

STM refer to the complex flow of stresses in structural members as axial elements in a truss. Concrete struts are resisting the compressive stress and reinforcing steel ties are resisting the tensile stress. The intersection regions

 

of struts and ties are called nodes. Struts, ties, and nodes as shown in Figure (28) are the three elements that consist the STM and they should be proportioned to resist the applied forces. The capacity of a STM is according to the lower bound theory of plasticity is always less than the structure's actual capacity provided the truss is in equilibrium and safe. Failure of a STM can be attributed to crushing of the struts, crushing of concrete at the face of a node, yielding of the ties, or anchorage failure of the ties. [4]

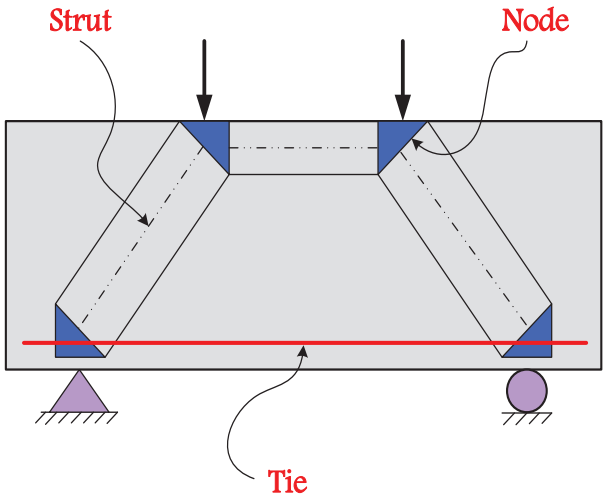


Figure 28. STM of Deep Beam.

STM in deep beams is represented by a structural truss as shown in Figure (28). Each type of the elements in a STM serves a unique purpose, but must be act in concert to describe accurately the behavior of a structure. STM consists of the following members and parts:

a. Struts: Struts are the compression members in the STM. Struts vary in shape. Most struts in a two dimensional STM are bottle-shaped, they spread laterally along their length. The lateral spreading of a bottle-shaped strut introduces tensile stresses transverse to the strut. Transverse reinforcement should be provided in order to control the cracking along the length of the strut that which occurs as a result of the tensile stresses. [4]
b. Ties: Reinforcing steel bars are set at tie locations in an STM. Ties are the tension members in the STM. The reinforcement should be distributed so that its centroid coincides with the tie location. Details such as distribution, bar spacing, and anchorage are factors that deserve the most consideration when selecting and placing the reinforcement. [4]
c. Nodes: Nodes form where struts and ties cross. Nodes are named according to the nature of the elements that frame into them. For example, the nodal zone where two struts and a tie intersect is referred to as a CCT node (C stands for compression and T stands for tension). Nodes are classified as CCC, CCT, CTT, or TTT. [4]

*4.2 Theoretical Results*

4.2.1 Capacity of the Tested Beams Using the STM

Ultimate load for six simply supported deep beams which tested under monotonic loading are calculated according to ACI 318 M-11Code. Table (12) and Figure (29) show the comparison between test results and the predicted values of the ultimate load. From Table (12), it can be noticed that the STM mentioned in ACI318M-11 Code underestimates the load capacity of deep beams. The mean value (X') for the ratio of analytical/test results of ultimate loads ($P_{An}/P_{Exp}$) is 0.75 where $P_{An}$ refers to ultimate loads obtained using analytical methods, the standard deviation (S.D.) is 0.13 and the coefficient of variation (C.O.V.) is 0.17.

 

Table 12.Comparison between Experimental Ultimate Loads and those Calculated Using STM of ACI 318M-11Code.

| *Beam No.* | $\rho_w$ | *Beam Type* | *SF Ratio* | *Ultimate Load($2V_n$) (kN)* | | *% $P_{An}/P_{Exp.}$* |
|---|---|---|---|---|---|---|
| | | | | *STM ACI 318M-11 Code* | *Experimental Value* | |
| **B1** | **0.003** | **Non –Hybrid (CC)** | **0%** | **332.60** | **370** | **0.90** |
| **B3** | **0.003** | **Non –Hybrid (FC)** | **1%** | **324.43** | **505** | **0.64** |
| **B5** | **0.003** | **Hybrid Beam** | **1%** | **325.01** | **480** | **0.68** |
| **B7** | **0.0** | **Hybrid Beam** | **1%** | **326.76** | **358** | **0.91** |
| **B9** | **0.004** | **Hybrid Beam** | **1%** | **409.91** | **510** | **0.80** |
| **B11** | **0.003** | **Hybrid Beam** | **2%** | **324.55** | **558** | **0.58** |

X' =0.75 S.D. = 0.13 C.O.V. = 0.17

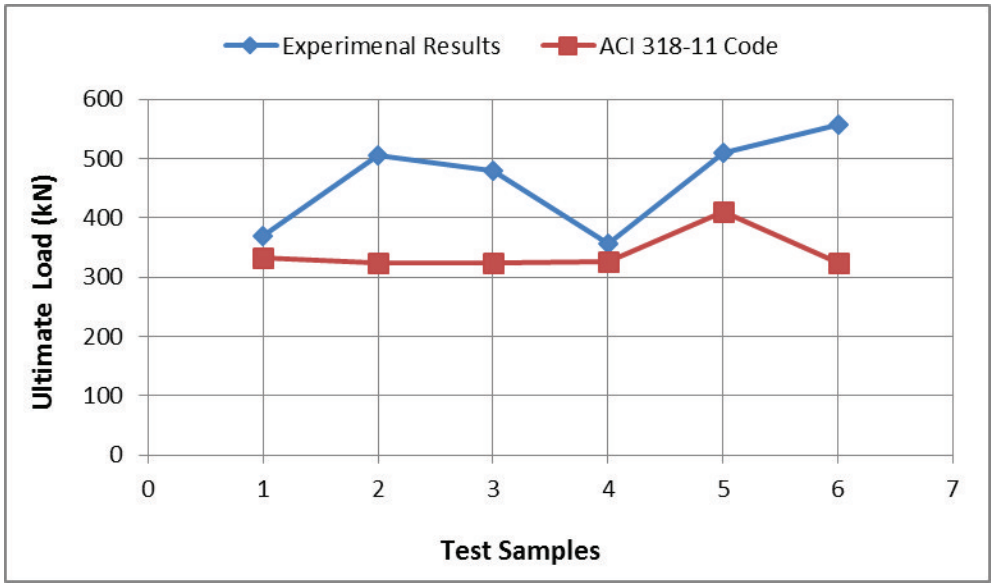


Figure 29. Comparison between Experimental Ultimate Loads and Analytical Loads Obtained Using the ACI 318 M-11Code.

4.2.2 Modified of STM Theory

Zhang and Tan in March (2007) [5], suggested a modified STM for calculation of shear strength of reinforced concrete deep beams based on a previous fulfillment reported by Tan and Cheng [6]. For simply supported reinforced concrete beams subjected to symmetric two point loads, from the structural analysis it is well known that the ultimate load (P) is equal to twice the shear force at the support.

$$P = 2Vn \quad (1)$$

The expression for calculated the shear strength $V_n$ according to Zhang and Tan [5], is as follows:

$$V_n = \frac{1}{\frac{4\sin\theta_s \cos\theta_s}{A_c f_t} + \frac{\sin\theta_s}{A_{str} f'_c}} \quad (2)$$

where;

$V_n$: shear strength of deep beams (N).

$A_c$ : is the beam effective cross- sectional area in $mm^2$, equals to $b_w$ $d_c$.

$d_c$: effective beam depth (mm).

$A_{str}$: cross-sectional area of the concrete diagonal strut in $mm^2$, equal to $w_s$ $b_w$.

$w_s$: effective width of the inclined strut (mm).

$b_w$: width of deep beam (mm).

$f_t$ : combined tensile strength of reinforcement and concrete (MPa).

$\theta_s$ : angle between the axis of the strut and the horizontal axis of the member.

It can be noted that the expression $f_t$ is the composite tensile strength included contributions from concrete and reinforcement (web and main bars), where;

$$f_t = f_{ct} + f_{st} \quad (3)$$

$f_{ct}$ : represents the contribution of concrete tensile strength.

 

$f_{st}$ : represents the contribution of steel reinforcement which consists of two parts, $f_{sw}$ from the web reinforcement and $f_{ss}$ from the longitudinal reinforcement as explain in equation (5.14).

$$f_{st} = f_{sw} + f_{ss} \quad (4)$$

Zhang and Tan suggested that the presence of web reinforcement in the strut restricts the inclined cracks from readily increase to every ends of the strut. Equation (5) shows the tensile contribution of web reinforcement at the interface of the nodal zone.

$$f_{sw} = \frac{A_{sw} f_{yw} \sin(\theta_s + \theta_w)}{A_c / \sin\theta_s} \quad (5)$$

For concerted cases of vertical and horizontal web reinforcement, equation (5.15) is reduced to:

$$f_{sw} = \frac{A_{sv} f_{yv} \sin 2\theta_s}{2A_c} + \frac{A_{sh} f_{yh} \sin^2 \theta_s}{A_c} \quad (6)$$

Where:

$A_{sv}$: total areas of vertical web reinforcement within the shear span ($mm^2$).

$A_{sh}$: total areas of horizontal web reinforcement within the shear span ($mm^2$).

$f_{yv}$: tensile yield strength of vertical web reinforcement (MPa).

$f_{yh}$: tensile yield strength of horizontal web reinforcement (MPa).

$\theta_s$: angle between the axis of the strut and the horizontal axis of the member.

$\theta_w$ : angle between the web reinforcement and the horizontal axis of beams at the intersection of the reinforcement and the diagonal strut.

The expression $f_{ss}$ refers to the contribution of bottom longitudinal steel, it can be obtained according to the following equation:

$$f_{ss} = \frac{4A_s f_y \sin\theta_s}{A_c / \sin\theta_s} \quad (7)$$

Where:

$A_s$: total areas of bottom longitudinal main reinforcement ($mm^2$).

$f_y$: tensile yield strength of main reinforcement (MPa).

Table (13) summarized the strength of the deep beams of the present investigation.

Table 13. Comparison between Experimental Ultimate Loads and those Calculated Using Modified STM Theory by N. Zhang and K.H. Tan [5].

| *Beam No.* | $\rho_w$ | *Beam Type* | *SF Ratio* | *Ultimate Load($2V_n$) (kN)* | | *% $P_{An}/P_{Exp.}$* |
|---|---|---|---|---|---|---|
| | | | | *Modified STM by Zhang and Tan* | *Experimental Value* | |
| **B1** | **0.003** | **Non –Hybrid (CC)** | **0%** | **598.58** | **370** | **1.62** |
| **B3** | **0.003** | **Non –Hybrid (FC)** | **1%** | **605.92** | **505** | **1.20** |
| **B5** | **0.003** | **Hybrid Beam** | **1%** | **609.59** | **480** | **1.27** |
| **B7** | **0.0** | **Hybrid Beam** | **1%** | **586.63** | **358** | **1.64** |
| **B9** | **0.004** | **Hybrid Beam** | **1%** | **617.16** | **510** | **1.21** |
| **B11** | **0.003** | **Hybrid Beam** | **2%** | **628.06** | **558** | **1.13** |

X'=1.3 S.D= 0.21 C.O.V= 0.15

From the above results, modified STM overestimates ultimate loads as compared to test results. The X' for $P_{An}/P_{Exp}$ ratio is 1.3, the S.D. is 0.21 and the C.O.V. is 0.15. These results are shown in Figure (30).

 

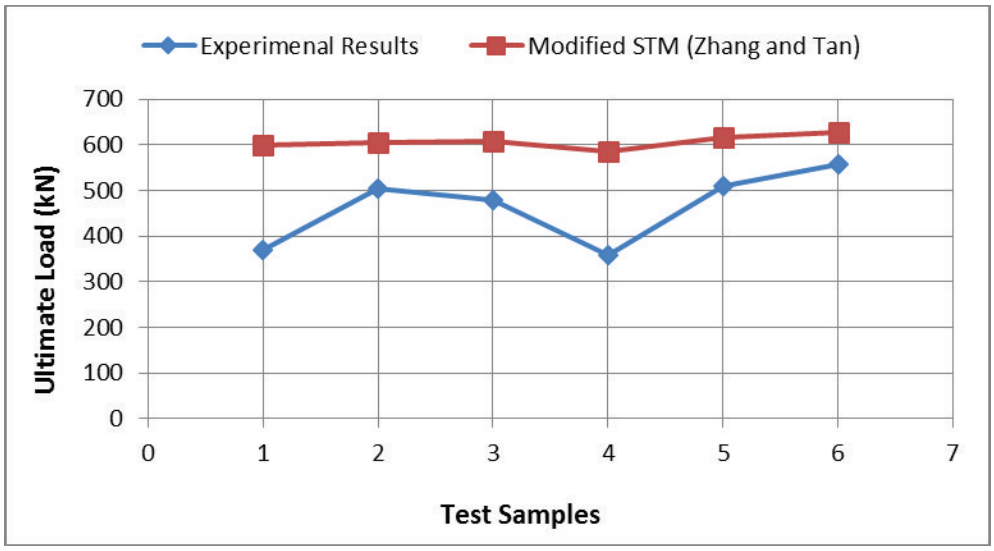


Figure 30. Comparison between Experimental Ultimate Loads and Analytical Loads Obtained Using the Modified STM Method.

4.2.3 Size Effect on the Capacity of Deep Beams Using the STM

Zhang and Tan in November (2007) [7] suggested the following modification to equation (2) for ultimate shear strength, taking into account the size effect.

$$V_n = \frac{1}{\frac{4\sin\theta_s\cos\theta_s}{Acf_t}+\frac{\sin\theta_s}{\upsilon A_{str}f_c'}} \quad (8)$$

The term $\upsilon$ refers to the efficiency factor accounts for the effect of strut geometry, and the effect of strut boundary conditions influenced by web reinforcement. The term ν is expressed as follows:

$$\upsilon = \xi \times \zeta \quad (9)$$

where;

$\xi$: efficiency factor for the effect of strut geometry.

$\zeta$: efficiency factor for the effect of strut boundary conditions influenced by web reinforcement. These parameters are expressed as follows:

$$\xi = 0.8 + \frac{0.4}{\sqrt{1+(l-w_s)/50}} \quad (10)$$

$$\zeta = 0.5 + \sqrt{k\, d_s/l_s} \leq 1.2 \quad (11)$$

Where,

$l$: length of strut in mm, as shown in Figure (31).

$d_s$: diameter of web steel bar, when web steel is not provided, $d_s$ is taken as the minimum diameter of bottom longitudinal steel bars.

$l_s$: maximum spacing of web steel intercepted by the inclined strut, when web steel is not provided, $l_s$ is equal to l.

$k = 0.5 \times \sqrt{\pi\, f_y/f_{ct}}$ is a material factor, when web steel is not provided, it is taken as half of the above value.

 

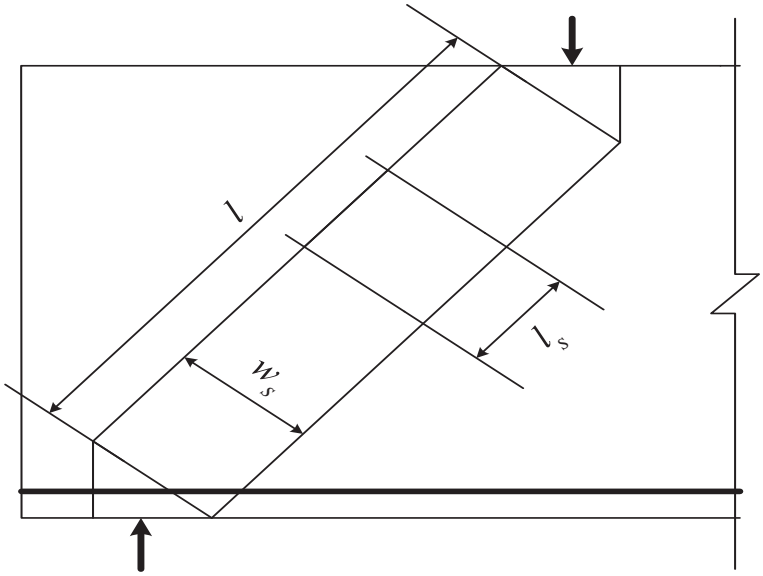


Figure 31. Strut Geometry and Strut Boundary Conditions.

Table (14) summarized the strength of the some deep beams of the present investigation which were tested under monotonic loading. The X' for $P_{An}/P_{Exp}$ ratio is 1.32, the S.D. is 0.21 and the C.O.V. is 0.16. These results are shown in Figure (32).

Table 14. Comparison between Experimental Ultimate Loads and those Calculated Using Equation (8).

| *Beam No.* | $\rho_w$ | *Beam Type* | *SF Ratio* | *Ultimate Load($2V_n$) (kN)* | | *% $P_{An}/P_{Exp.}$* |
|---|---|---|---|---|---|---|
| | | | | *Modified STM Equation (8)* | *Experimental Value* | |
| **B1** | **0.003** | **Non –Hybrid (CC)** | **0%** | **607.54** | **370** | **1.64** |
| **B3** | **0.003** | **Non –Hybrid (FC)** | **1%** | **553.19** | **505** | **1.10** |
| **B5** | **0.003** | **Hybrid Beam** | **1%** | **613.21** | **480** | **1.28** |
| **B7** | **0.0** | **Hybrid Beam** | **1%** | **562.28** | **358** | **1.57** |
| **B9** | **0.004** | **Hybrid Beam** | **1%** | **620.46** | **510** | **1.22** |
| **B11** | **0.003** | **Hybrid Beam** | **2%** | **625.25** | **558** | **1.12** |

X'=1.32 S.D=0.21 C.O.V=0.16

 

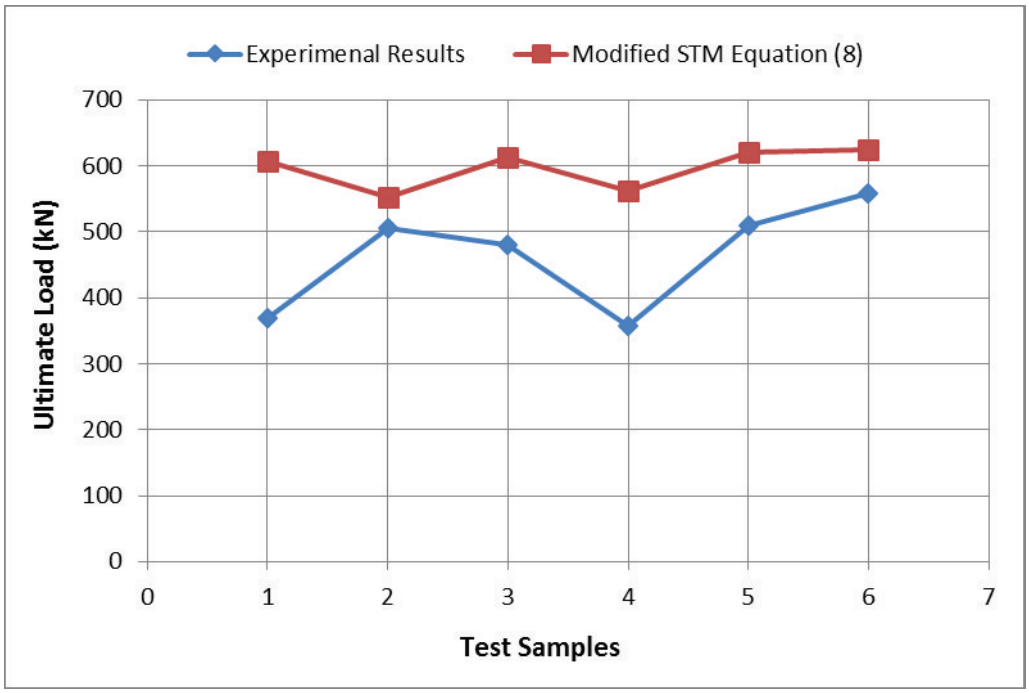


Figure 32. Comparison between Experimental Ultimate Loads and Analytical Loads Obtained Using Equation (8).

## 5. Comparison between Ultimate Loads Obtained Using Different Analytical Methods and Experimental Values.

Through the analytical methods presented in the previous articles, it was to obtain different values of ultimate load as compared with the experimental data of the reinforced concrete simply supported deep beam that which tested under monotonic load in this work. These differences in results are shown in Table (15), Figure (33).

Table 15. Comparison between Ultimate Loads Obtained Using Experimental Results and Different Analytical Methods.

| *Beam No.* | *$P_{Exp.}$ Experimental (kN)* | *$P_{An.}$* | | |
|---|---|---|---|---|
| | | *STM ACI 318M-11 Code (kN)* | *Modified STM by Zhang and Tan (kN)* | *Modified STM Using Equation (8) (kN)* |
| **B1** | **370** | **332.60** | **598.58** | **607.54** |
| **B3** | **505** | **324.43** | **605.92** | **553.19** |
| **B5** | **480** | **325.01** | **609.59** | **613.21** |
| **B7** | **358** | **326.76** | **586.63** | **562.28** |
| **B9** | **510** | **409.91** | **617.16** | **620.46** |
| **B11** | **558** | **324.55** | **628.06** | **625.25** |
| **X'($P_{An}/P_{Exp.}$)** | | **0.75** | **1.3** | **1.32** |
| **S.D. ($P_{An}/P_{Exp.}$)** | | **0.13** | **0.21** | **0.21** |
| **C.O.V. ($P_{An}/P_{Exp.}$)** | | **0.17** | **0.15** | **0.16** |

 

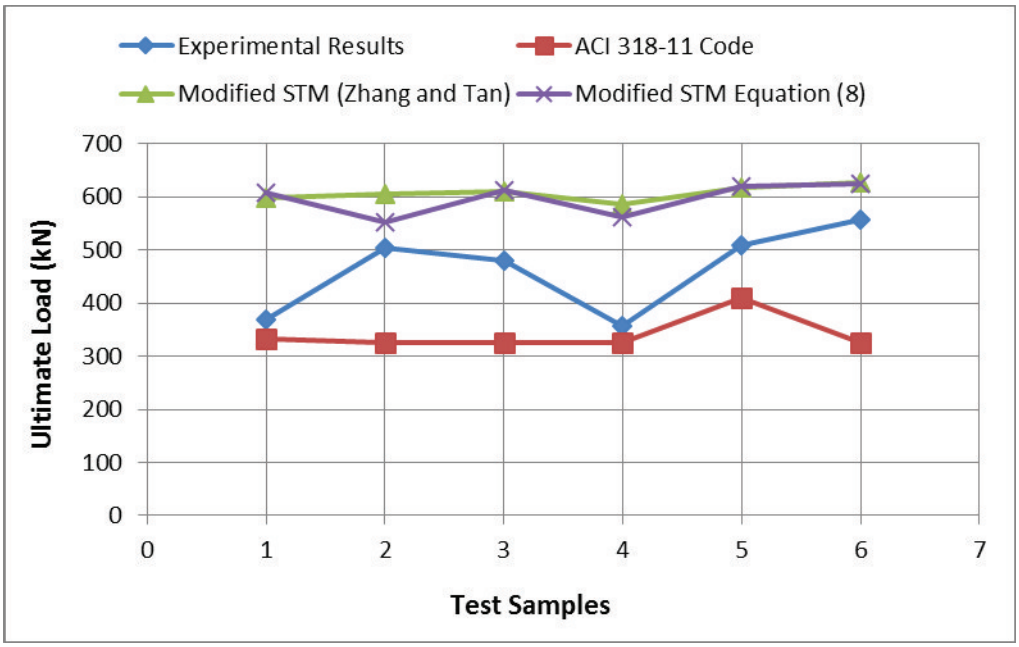


Figure 33. Ultimate Loads Obtained Using Different Experimental and Analytical Methods.

## 6. Conclusion

*6.1 Experimental Phase*

1. The percentages decrease in ultimate load according to repeated loading for non-hybrid deep beams of CC and FC is convergent which are (20.81% and 18.81%), respectively.
2. The percentages decrease in ultimate load according to repeated loading which have SF ratio of (1% and 2%) as variable is convergent (27.08% and 25.09%), respectively.
3. The percentages decrease in ultimate load according to repeated loading which have web reinforcement of (0.003 and 0.004) as variable is convergent (27.08% and 23.53%), respectively.
4. The percentages decrease between the hybrid deep beams without web reinforcement when subjected to monotonic and repeated loading is of negligible value (1.96%).
5. The mean value of the percentages decrease of beams subjected to monotonic and 70% repeated loading is (23.06%) excluding the percentage decease of beams without web reinforcement since it is far from all other values (abnormal).
6. The results reveal that the presence of SF at the middle portion (portion of zero shear) under monotonic loading is not that important. The increase in ultimate load of beam cast entirely with FC is 5.21% as compared with that of hybrid deep beam with FC only at its shear spans. Also, the increase in ultimate load of FC deep beam is 36.49% as compared with CC deep beam.
7. It can be found that the hybrid beam with FC only at its shear spans fails under repeated loading in load higher than non-hybrid beam cast from CC by (19.45%), while beam which was cast entirely with FC (SF1%) fails in load significantly higher than the CC beam by 39.93% and hybrid beam with FC only at its shear spans by17.14%.
8. The ultimate load increases as the SF ratios increase. It was found that when adding SF to the shear spans of the tested deep beams under monotonic system loading by ratios ranged from (0% to 2%), the ultimate load increases from 29.73% to 50.81%, as compared with beam without SF. It was found that SF ratio in hybrid beams under repeated loading is significant. The capacity of hybrid deep beams with ratio of SF 2% and 1% were increased by about 42.66% and 19.45%, respectively as compared with deep beams without SF.
9. The ultimate load for deep beams that which tested under monotonic loading increases from 34.08% to 42.46%, respectively as the ratio of $\rho_w$ increased from (0 to 0.003) and from (0 to 0.004). while when tested similar deep beams under repeated loading, it can be seen that there is no increase in the value of ultimate load as $\rho_w$ increase from (0 to 0.003) which is minimum reinforcement ratio while there is an increase in ultimate load value of (11.11%) as $\rho_w$ increased from (0 to 0.004).

*6.2. Analytical Phase*

1. Strut and Tie Model presented in Appendix A of ACI 318M-11 Code results in conservative values of

 

ultimate loads as compared with the corresponding experimental ones. It can be noticed that the STM underestimates the load capacity of deep beams. The mean value (X') for the ratio of analytical/test results ultimate loads ($P_{An}/P_{Exp}$) is 0.75 where $P_{An}$ refers to ultimate loads obtained using analytical methods, the standard deviation (S.D.) is 0.13 and the coefficient of variation (C.O.V.) is 0.17.

2. The modified developed by (Zhang and Tan in March 2007) gives capacities, which overestimate values for deep beam with web reinforcement ratios more than minimum ($\rho_w$ =0.004) and for hybrid deep beam with SF ratio 2% in shear spans. Also, the expression results in underestimated values for the beam without web reinforcement ($\rho_w$ =Zero). The expression gives capacities which are convergent values for deep beams non-hybrid (CC), non- hybrid (FC) and hybrid beam with SF ratio 1% (B5). The X' is 1.3, the S.D. is 0.21 and the C.O.V. is 0.15.
3. The modified expression developed by (Zhang and Tan in November 2007), that includes the effect of size factor, gives capacities for deep beam, which overestimate values for deep beam with web reinforcement ratio more than minimum ($\rho_w$ =0.004). Also, the expression results in underestimated values for deep beam without web reinforcement ($\rho_w$ =Zero). The expression, also gives capacities which are convergent values for deep beams non-hybrid (CC), non-hybrid (FC), hybrid deep beam with SF ratio 1% and 2% in shear spans. The X' is 1.32, the S.D. is 0.21 and the C.O.V. is 0.16.

## 7. References

1- ACI Committee 318M-318RM, "***Building Code Requirements for Structural Concrete and Commentary***", American Concrete Institute, Farmington Hills, Michigan, 2011. 503 pp.
2- S.Y. Noh, C.Y. Lee and K. M. Lee, ***"Deep Beam Design Using Strut-Tie Model"***, University at Ansan, Korea.
3- B. S. Maxwell and J. E. Breen, ***"Experimental Evaluation of Strut-and-Tie Model Applied to Deep Beam with Opening "***, ACI Structural Journal, Vol.97, No.1, 2000, pp. 142-148.
4- D. Birrcher, R. Tuchscherer, M. Huizinga, O. Bayrak, S. Wood and J. Jirsa, ***"Strength and Serviceability Design of Reinforced Concrete Deep Beams"***, CTR Technical Report, December, 2008.
5- N. Zhang, and K.H. Tan, ***"Direct Strut-and-Tie Model for Single Span and Continuous Deep Beams"***, Science Direct, Engineering Structures Journal, Vol.29, March, 2007, pp. 2987-3001.
6- Tan, K. H., and Lu, H. K., "***Shear Behavior of Large Reinforced Concrete Deep Beams and Code Comparisons***", ACI Structural Journal, Vol. 96, No. 5, September-October, 1999, pp. 836-845.
7- N. Zhang, and K.H. Tan, ***"Size Effect in RC Deep Beams: Experimental Investigation and STM Verification"***, Science Direct, Engineering Structures Journal, Vol.29, November, 2007, pp. 3241-3254.